

Development of Hybrid Wolf Optimization with Faster Mask RCNN to Predict the Healthcare System at an Earlier Stage

¹Z. John Bernard, ²Dr. C. Chandrasekar

Submitted: 08/02/2024 Revised: 13/03/2024 Accepted: 19/03/2024

Abstract: Diabetic Retinopathy (DR) is a retinal complication brought by the metabolic disorder diabetes, that is, the four primary causes of blindness worldwide. It can be difficult to diagnose DR because there are typically no obvious symptoms before the onset. If the need for DR identification is not effectively automated, the healthcare sector may suffer negative effects. As a result, we want to create a system for classifying DR samples that is both automated and economical. In this paper, we proposed the Faster Mask Recurrent Convolutional Neural Network (FM-RCNN) method for the identification of retinal images to classify DR lesions. We produce the dataset annotations needed for model training after pre-processing. The representative set of key points is then computed by introducing MD-ResNet at the FM-RCNN feature extraction level. After localizing and classifying the input sample into five categories, the FM-RCNN completes the process. With a 97.2% accuracy rate, the newly developed methodology excels, according to rigorous tests on a Kaggle dataset consisting of 88,704 visuals. We have contrasted our method with cutting-edge methods to demonstrate its robustness in terms of DR classification & localization. Additionally, we validated the Kaggle data across datasets and both the training and testing phases of the APTOS datasets and produced outstanding results.

Keywords: Diabetes Retinopathy; Early prediction; Faster Mask RCNN; Classifications; Accuracy

1. Introduction

Numerous researchers have put a lot of effort into the study of DR. Medical field and Machine Learning (ML) are related in the research work, which demonstrates that numerous machine learning implementations have been used by researchers to identify the DR [1-2]. Due to the size of the field, there are still open spots where research can be conducted to produce accurate results [3]. Following is a discussion of some of the related works mentioned in the literature review. To identify anomalies in retinal fundus images, the author used a computer-based technique. To improve image quality, the author's proposed methodology first employs a noise removal process [4]. Imaging of the optic disc, statistical extraction from exudates, and blood vessel tracing are additional tasks [5]. Following feature extraction is completed, Mild, moderate, and severe diabetic retinopathy are classified using machine learning techniques.

People with a history of diabetes mellitus are more likely to experience DR [6]. Blood leakage is triggered by high blood glucose levels and additional blood vessel fluids in the retina. It is the reason why diabetic subjects experience vision loss [7]. Proliferative and Non-

Proliferative DR are the two primary stages of DR [8]. The following major lesions are being taken into consideration for grading: Blood vessels, Microaneurysms, Exudates, and Hemorrhage. PDR is the term used to describe the advanced stage with neovascularization, and the DR stage with any of these lesions is known as NPDR. It's challenging to recover from DR when it's severe. Complete vision loss will result from it [9-11]. It is extremely important to lessen its prevalence globally. To identify the signs of DR, various methods have been used. But the methods for feature extraction are difficult to master. Maximizing the accuracy of the feature extraction for DR classification is crucial to cut back on computation time and costs [12]. To present a straightforward, the proposed work's objective is to use all these details to extract features from Convolutional Neural Network (CNN) for improved classification and combine it with classifiers of ML.

The implementation of CNN is discussed in this paper. Neural networks for classification and convolution layers for feature extraction make up its fundamental components [13]. The convolution layer, the first and second layers of CNN, uses kernels that are convolved with the image to detect necessary patterns, shapes, or colors [14]. Convolution layers that extract observable features from an image make up the first layers of the CNN algorithm. Convolution with kernels is used in the CNN's subsequent layers of processing to extract more ethereal and hidden features from the output of the initial

¹Research Scholar, Department of Computer Science, Bharathiar University, Coimbatore, Tamilnadu, India.

²Assistant Professor, Department of Computer Science, Government Arts and Science College for women, Coimbatore, Tamilnadu, India

¹bernard_802000@yahoo.com, ²chandrasekar2000@gmail.com

layers [15]. With neural networks, the final layer processes the image's weighted impact of all the features. The CNN architecture used in this study was created from the ground up to optimize the detection of diabetic retinopathy using fundus images. and for comparison, an additional 3 different pre-trained models are used [16].

2. Related Works

Two major issues with automated grading [17]. Specificity and getting the desired precision offset are the first ones. Again, it is much more difficult to achieve the same grade when five classes are taken into consideration in this work. The overfitting of the neural network comes in second. The system's training algorithm is particularly connected to these two. Modern Deep Learning (DL) methods called CNN have made significant advancements in the checking process and numerous disciplines, such as medical imaging, and the detection of objects. With a clear CNN architecture, the task at hand is to address the feature extraction stage's problems [18]. For DL algorithms to function, a large database must be accessible. For classification, ML classifiers can be used to address this issue, and CNN to accurately classify diseases by extracting tiny features from fundus images [19]. As a result, efficient and precise automated methods can take the place of labor-intensive feature extraction techniques.

The use of an Artificial Neural Network (ANN) to measure the severity level of DR automatically is explained. The retinal fundus image is used to determine the presence of lesions such as exudates, hemorrhage, Blood vessels, and MAs [20]. To categorize DR into mild, moderate, and severe cases, afterward, a multilayer feed-forward neural network was used to process the lesions. The technique uses a two-stage CNN to find on a fundus image, there are unusual lesions. [21]. Here, the DR was graded and the location and lesion type in the image were identified. Using ANN, the four lesions are classified into mild, moderate, and severe categories based on features like area, perimeter, and count [22]. Using Principal Component Analysis (PCA), they were able to choose a better feature. The classification process was then carried out using one rule classifier and a backpropagation neural network.

The project's foundation is the fundus examination photographs with various lighting and field-of-view settings [23]. They used various classifiers to grade the DR, including the Gaussian Mixture Model (GMM), AdaBoost, Support Vector Machines (SVM), and k-Nearest Neighbor (k-NN) [24-26]. k-NN and GMM outperformed the competition, by their analysis of performance, fewer features are required for lesion classification; therefore, Using the feature ranking method was the main responsibility [27]. Haralick and ADTCWT are combined to create a new feature extraction technique. To grade DR, the classifier is then fed the chosen features. Grading was proposed using a three-stage model. To increase the effectiveness of the classification, they used a hybrid classifier. To train the classifier's weights, a Genetic Algorithm (GM) was employed. The outcomes demonstrated that the system accurately classified the severity of all NPDR lesions and detected them all.

3. Proposed Method

A new kind of FM-RCNN is constructed by the framework's second element that was introduced. A CNN framework is the first of two sub-modules in this module and the training element is the additional factor, which uses the important information derived from the CNN model to carry out training of the FM-RCNN. The spot where the lesion is in the picture sample and the input image are the two types of input that FM-RCNN accepts. The effectiveness of the proposed technique is depicted in Figure 1. First, the selected CNN model receives an input sample along with the Annotation's Bounding Box (ABB). The CNN key points' region of interest is recognized by the ABB. Key points from training samples that have been reserved are nominated using these ABB. A classifier and an estimator are created by the FM-RCNN. for a regressor for the specified regions based on the computed features. Objects are given predicted classes by the classier modules and to identify which image's lesion is where it is in each, the regressor component acquires the ability to pinpoint potential ABB coordinates. According to metrics used in the CV field, accuracy is finally estimated for each unit.

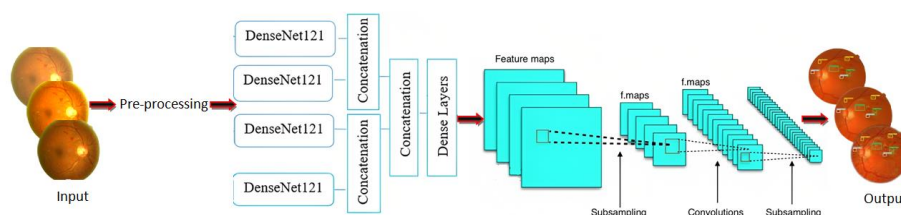
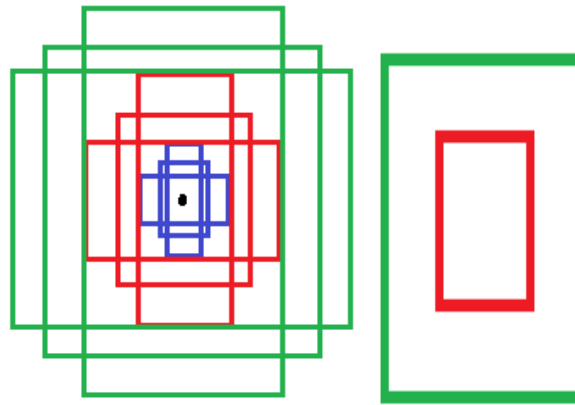


Fig 1: A custom FM-RCNN model's architecture

The portion of the structure that has been improved is indicated by the small, dashed box in the top half of the illustration, the Region Proposal Network (RPN) layer. For one target on the feature map in the original FM-RCNN, the RPN layer offers nine anchors. These nine anchors, which are displayed as a collection of rectangular boxes with three sizes (128, 256, and 512) and three aspect ratios (1:1, 1:2, and 2:1), are designed for data sets with multiple target sizes, as shown in



*a)Initial nine anchors (b) Enhanced 2 anchors

Fig 2: FM- RCNN Anchors

Figure 3 illustrates the enhanced ResNet structure, where the network's end is added with a dilated convolution module. Additionally multi-level fused are the additional

Figure 2 (a). Extra anchors, however, affect the speed of detection and lead to variations in the results for macular targets. With only a 1:1 aspect ratio, the nine anchors are reduced to two 80x80 and two 160x160 anchors, as shown in Figure 2 (b). To improve the accuracy of macular area localization and reduce the computational load on the new anchors, redundant anchors are eliminated.

dilated convolution layers and residual network layers; The MDResNet structure places the fusion algorithm immediately beneath the convolutional layers.

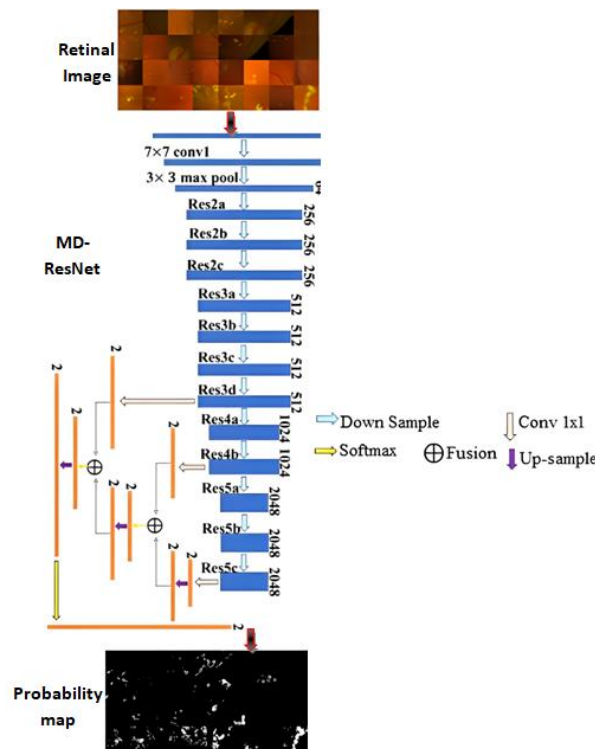


Fig 3: MD-ResNet network structure

Preprocessing

Our data includes a variety of artifacts, including blurred pictures, noise, and overexposed or underexposed pictures. This could produce subpar classification

outcomes. As a result, before entering the samples into CNNs, we pre-process their data.

$$G(i, j) = \frac{1}{2\pi\sigma^2} \exp\left(-\frac{i^2+j^2}{2\sigma^2}\right) \quad (1)$$

where the horizontal and vertical axes' distances from the origin are represented by the letters i and j , respectively, and σ is the variance. Following that, we apply Equation (2) to the blurred image to subtract the local average color.

$$X'(i,j) = X(i,j) - (G(i,j) * X(i,j)) \quad (2)$$

The contrast-corrected image is represented $X'(i,j)$, $X(i,j)$, and $(G(i,j) * X(i,j))$, The original image and the original image after applying a Gaussian filter, respectively. Certain portions of the image in the original dataset can be removed without changing the results. So, from the input image, we crop these areas. Cropping pictures helps with computation efficiency while also improving classification performance.

However, because it makes use of the RPN, FM-RCNN's functionality is altered to proactively develop framework-integrated region proposals. By using RPN instead of the Edge Boxes algorithm, FM-RCNN achieves this. FM-RCNN has significantly less computational complexity than the edge box method for

producing region proposals [28]. Simply put, RPN determines the order of the anchor boxes and displays those that contain regions of interest most frequently. As a result, FM-RCNN's region is faster and more responsive to input samples than before, proposal generation. The FM-RCNN produces two different types of outputs: (i) showing the class connected to each object in classification and (ii) Location data for ABB.

The issue of the top-level key points lacking target position information can be somewhat improved by using MD-ResNet to present the complex transformations. The number of parameters is kept to a minimum with MD-ResNet, making them economical. Additionally, MD-ResNet supports the propagation of key points and allows for better classification of lesions and digits by encouraging their reuse. To use the MD-ResNet as an extractor of features for the FM-RCNN in this paper, we have done so. Table 1 displays the FM-RCNN's training parameters. The algorithm displays the specifics of our proposed approach.

Table 1: Training parameters

Parameters	Value
Epochs	22
Learning rate	0.002
Threshold IOU	0.91
Threshold (Matched)	0.6
Threshold (Unmatched)	0.6

Four steps make up Lesion classification using FM-RCNN as the primary process. For MD-ResNet to create the feature map, the input sample and annotation are first provided, subsequently, the RPN component receives the calculated key points as input, to learn more about the region's proposed features. The third step involves creating by utilizing the calculated feature map, the proposed feature maps, which are done by the ROI pooling layer and RPN unit suggestions, and the Convolutional layer are presented here. The final step displays each lesion's class using the more sophisticated unit. The precise location of the referred to is shown using the ABB produced by the ABB regression.

Algorithm 1: DR recognition procedures using a customized FM-RCNN

Step 1: Start

Step 2: Input: Position (annotation) – Samples coordinates in BB, NX – Samples (all) with DR

Step 3: Output: RoI – Position (Lesion). (Model based on FM-RCNN)

Step 4: Assign [340 X 240] the size of the image

Step 5: Assign the ABB estimation of Annotation to NX AnchorsEstimation (NX, annotation)//

Step 6: Construct the custom CFstDenseNet-65 to FM-RCNN (imageSize, α)

Step 7: Partition the data set into Testing (ts) and training (tr)

Step 8: for each sample x in tr

{

Step 9: Extract DenseNet-65 key points from NX

}

Step 10: Train the model over NX and the training time measured

Step 11: $\eta_{dense} \leftarrow \text{PreLesionLoc}(nx)$

Step 12: $Ap_dense \leftarrow Evaluate_AP (CFstDenseNet-65, \eta_dense)$

Step 13: For each X in ts

{

Step 13.1: Calculate trained model $\epsilon \rightarrow \mu X$

Step 13.2: BB updated and predicted

Step 13.3: Display BB image on its classification

Step 13.4: $z \leftarrow z [BB]$

}

Step 14: Update the model

Step 15: end

Utilizing the Intersection over Union (IOU) as shown in Figure 4 (a), the proposed method is evaluated. The

approximately rectangular with DR lesions is shown as Y , and the ground truth rectangle is shown as X . IOUs are considered valid when their value exceeds 0.5, the initial choice for lesions to be identified. If the value is less than 0.5, it is decided whether it is. The most used to assess the accuracy of object detectors is the Average Precision (AP). Figure 4 (b) illustrates how precision can be explained geometrically and is dependent on the concept of IOU in our framework. As seen in Figure 5, the Dense block is a crucial part of MD-ResNet. An alteration that is nonlinear H , which includes all of the operations, i.e., A 1×1 convolution layer is used to reduce multiple channels, and a 3×3 ConvL is used for feature restructuring. Finally, the $L + 1$ layer's output is $ss(k_0 + 2k)$.

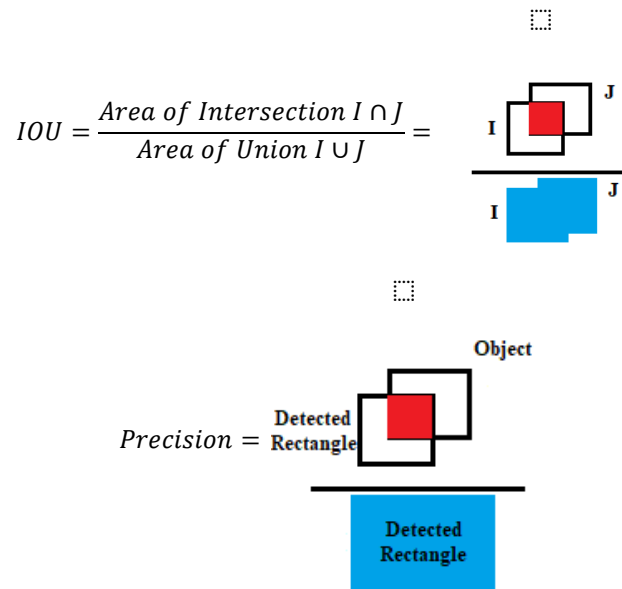


Fig 4: (a) Venn diagram (IOU) (b) Precision calculation

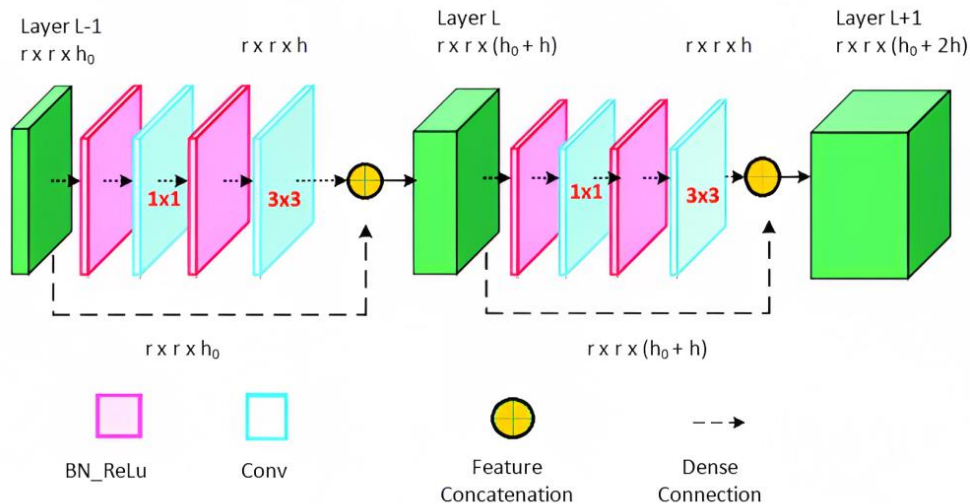


Fig 5: Dense Block architecture for FM-RCNN

The number of FPs will dramatically increase following several dense connections, to reduce a dense block's previous feature dimension, the transition layer (TL) is added. Figure 6 displays the TL structure, which reduces the size of FPs by starting with BN and a 1x1 ConvL, then adding a 2x2 average pooling layer. Where pool represents average pooling and t indicates the number of channels overall.

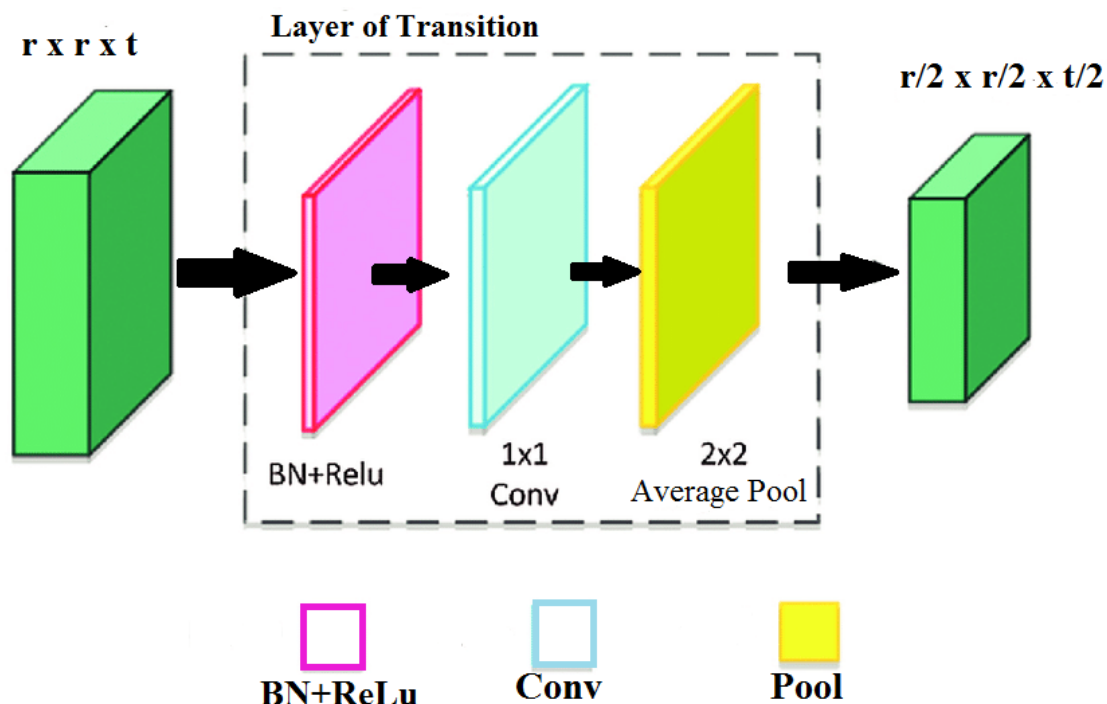


Figure 6: Architecture of transition layer

The deep learning-based method FM-RCNN does not rely on techniques like selective search to generate its proposal. As a result, the network receives the input sample with annotation where the digit location and associated class are displayed using an ABB that is computed directly with this technique, we make use of the Kaggle DR image database. 88704 images total, divided into two sets, are used as training images. The data about the DR severity level is provided in a label.csv file. Various cameras were used in several clinics over time to collect the samples for the database.

4. Result and Discussion

When compared to base models, the proposed MD-ResNet method's detection accuracy is evaluated. In this section, we display the simulation outcomes for

DenseNet-65, ResNet, and EfficientNetB5. For DR image classification, the results are shown in terms of accuracy. According to trainable parameters, Tab. 2 compares the three models that were used in DR image classification is used in this work, loss, total parameters, and model accuracy.

the EfcientNet-B5 has the most model parameters. This is because the structure of MD, the strength of very deep and wide networks is not all that ResNet is dependent on, rather, reusing model parameters is made effective by them. Consequently, the total number of model parameters is significantly reduced. For instance, DenseNet-65, or 65 layers deep, is the architecture of MD-ResNet that is being considered in this work. Like DenseNet-65, the ResNet used in this study has 50 layers but significantly more parameters.

Table 2: Table of equivalents of various characteristic

Parameter of evaluation	Proposed System	EfficientNet-B5	ResNet
Total parameters	7054712	28190304	25699015
Trainable parameters	6962987	28190304	25638913
Non-trainable parameters	85231	0	53122
Test loss	0.12	0.218	0.20
Test accuracy	0.988	0.7995	0.95

In MD-ResNet, there are only a few trainable parameters, i.e., 6, 958, 900, compared to ResNet's and EfficientNet-B5's trainable parameters. The training period for the previous deep network as a result. According to Table 3 of our analysis, the MD-ResNet performs better

at classifying data than the other methods. 95.6% of the images depicting DR-affected human retinas are classified correctly by MD-ResNet. Contrarily, EfficientNet-B5 and ResNet have classification accuracy rates of 94.5% and 90.4%, respectively.

Table 3: Comparative analysis

Model	Accuracy
AlexNet	89.91
VGG	95.7
GoogleNet	93.38
ResNet	90.42
DenseNet-121	92.41
EfficientNet-B5	94.6
Proposed system	97.4

4.1 DR Lesions Using FM-RCNN

The infected regions are regarded as an example of success in localizing the DR signs, in contrast, the healthy portions that are still present are known as the bad example. IOU, a score below this one, less than the threshold score of 0.5, classifies the correlated area, taking the location's history or reputation into account. Lesions are also defined as areas with an IOU value greater than 0.5. The Custom FM-RCNN's localization results, as shown in Figure 7 had to be assessed over a

confidence level using retinal sample data. The evaluation's findings show a higher value that ranges between 0.89 and 0.99. By using the precision and mean IOU across all samples of the test database, the results of the presented methodology are examined. According to Table 4, the proposed framework was successful in achieving a precision of 0.974 and means IOU average values of 0.969. By using FM-RCNN based on DenseNet-65, our proposed method achieves better results due to the precise localization of lesions.

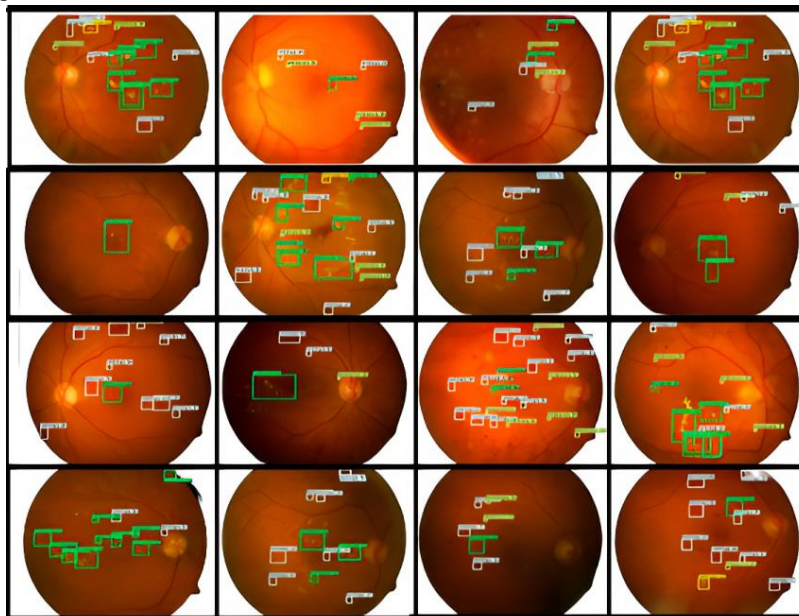


Fig 7: Results of tests using a customized FM-RCNN to identify DR lesions

Table 4: The effectiveness of the proposed method on the Kaggle database

Lesions (DR)	IOU Mean	Precision
Hard exudates	0.992	0.98
Soft exudates	0.975	0.963
Micro aneurysms	0.993	0.87
Hemorrhages	0.929	0.97

Through the experiments, the introduced framework's results are examined stage-by-stage. The lesions of the DR were accurately localized and classified by FM-RCNN. In Table 5, the outcomes of the classification of the DR are shown in terms of error rate, precision, accuracy, F1-score, and recall. The error rate, precision, accuracy, F1-score, and recall averaged out to 0.034, 0.974, 0.972, 0.966, and 0.96 for the technique that was presented. Good classification results from the correct

computation of DenseNet65 key points, which practically displays each class. Additionally, a weak correlation between the Mild DR and No classes is discovered, but neither class is unrecognizable. As a result, our method displays the most recent DR classification effectiveness, demonstrating the stability of the network that was presented, thanks to efficient key point computation. Figure 8 depicts the confusion matrix.

True Class	No DR	97%	5%	0	0	0
	Mild	5%	93%	3%	0	3%
	Moderate	0	0	98%	2%	2%
	Severe	0	2%	0	99%	0
	Prolific	0	4%	0	0	96%
		No DR	Mild	Moderate	Severe	Prolific
		Predicted Class				

Fig 8: Results of tests on a unique FM-RCNN

Table 5: Effectiveness of the proposed methodology on a stage-by-stage basis

Stage level	Accuracy	F1-Score	Recall	Error-rate	Precision
No DR	0.98	1	0.918	0	0.925
Mild	0.930	0.922	0.941	0.080	0.989
Moderate	0.98	0.995	1	0.008	0.981
Severe	0.993	0.956	0.955	0.048	0.990
Proliferative	0.983	0.964	0.98	0.036	0.994

4.2 Comparative Analysis

In the current study, we reported the outcomes of a 10-time computer simulation. We used a 30% to 70% data split for testing and training in each run, chosen at random. Next, we looked at the typical results for the performance assessment metrics. While similar methods achieved an average accuracy of 84.735, the proposed method attained an accuracy of 97.2%. We can state that the performance increase from our technique was 12.46%.

In Figure 9, we have drawn a box plot to assess the cross-dataset. The median, quartiles, and outliers of the number line show how accurately test and train results are distributed. The graph shows that we trained with a 0.981% average accuracy and test results of 0.975% show that our proposed work performs better than both the unknown and known samples. This leads to the conclusion that the proposed framework is resistant to classification and DR localization.

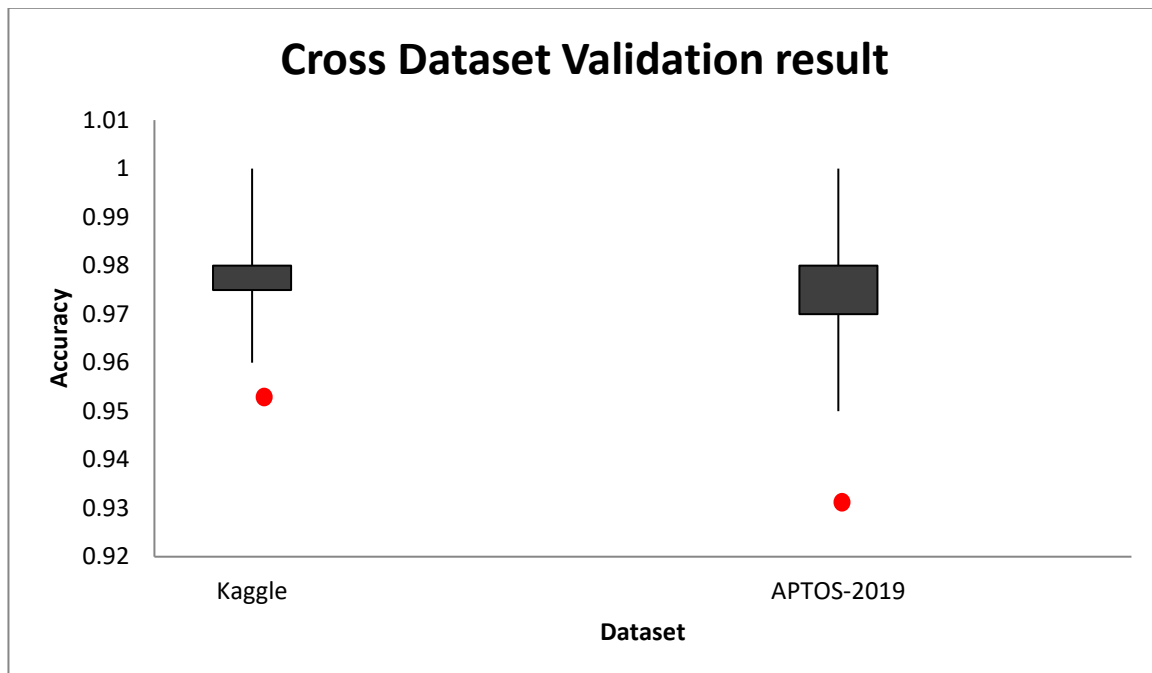


Fig 9: Validation across datasets outcomes

5. Conclusions

In this study, we developed a unique FM-RCNN framework to enumerate the different DR levels and accurately presented a program for classifying lesions. To be more specific, the supplied sample's deep features that FM-RCNN trained onto recognize DR by using MD-ResNet for the purpose of computing. Retinal images can be efficiently classified into five classes using the proposed method. Our approach is also resistant to a variety of artifacts. Our approach outperforms the newest approaches, according to reported results. We intend to improve our method in the future to treat additional eye-related conditions.

References

- [1] Das, S. K., Roy, P., & Mishra, A. K. (2022). DFU_SPNet: A stacked parallel convolution layers-based CNN to improve Diabetic Foot Ulcer classification. *ICT Express*, 8(2), 271-275.
- [2] Das, S. K., Roy, P., & Mishra, A. K. (2022). Oversample-select-tune: A machine learning pipeline for improving diabetes identification. *Concurrency and Computation: Practice and Experience*, 34(5), e6741.
- [3] Alatrany, A. S., Hussain, A., Alatrany, S. S., & Al-Jumaily, D. (2022). Application of Deep Learning Autoencoders as Features Extractor of Diabetic Foot Ulcer Images. In *International Conference on Intelligent Computing* (pp. 129-140). Springer, Cham.
- [4] Garikapati, P., Balamurugan, K., Latchoumi, T. P., & Malkapuram, R. (2021). A Cluster-Profile Comparative Study on Machining AlSi 7/63% of SiC Hybrid Composite Using Agglomerative Hierarchical Clustering and K-Means. *Silicon*, 13, 961-972.
- [5] Alshayegi, M. H., & Sindhu, S. C. (2023). Early detection of diabetic foot ulcers from thermal images using the bag of features technique. *Biomedical Signal Processing and Control*, 79, 104143.
- [6] Mishra, A. K., Roy, P., Bandyopadhyay, S., & Das, S. K. (2022). A multi-task learning based approach for efficient breast cancer detection and classification. *Expert Systems*, 39(9), e13047.
- [7] Santos, F., Santos, E., Vogado, L. H., Ito, M., Bianchi, A., Tavares, J. M., & Veras, R. (2022, June). DFU-VGG, a Novel and Improved VGG-19 Network for Diabetic Foot Ulcer Classification. In *2022 29th International Conference on Systems, Signals and Image Processing (IWSSIP)* (pp. 1-4). IEEE.
- [8] Bloch, L., Brüngel, R., & Friedrich, C. M. (2021, September). Boosting EfficientNets Ensemble Performance via Pseudo-Labels and Synthetic Images by pix2pixHD for Infection and Ischaemia Classification in Diabetic Foot Ulcers. In *Diabetic Foot Ulcers Grand Challenge* (pp. 30-49). Springer, Cham.
- [9] Liu, B., Wang, H., Wang, X., Long, J., Zhuang, X., Ji, X., ... & Zhao, S. Four-gene signature based on machine learning filtration could predict prognosis of patients with breast cancer. *Expert Systems*, e13157.
- [10] Santos, E., Santos, F., Dallyson, J., Aires, K., Tavares, J. M. R., & Veras, R. (2022, July). Diabetic Foot Ulcers Classification using a fine-tuned CNNs Ensemble. In *2022 IEEE 35th International*

Symposium on Computer-Based Medical Systems (CBMS) (pp. 282-287). IEEE.

- [11] Harahap, M., Anjelli, S. K., Sinaga, W. A. M., Alward, R., Manawan, J. F. W., & Husein, A. M. (2022). Classification of diabetic foot ulcer using convolutional neural network (CNN) in diabetic patients. *Jurnal Infotel*, 14(3), 196-202.
- [12] M. Anand, N. Balaji, N. Bharathiraja, A. Antonidoss, A controlled framework for reliable multicast routing protocol in mobile ad hoc network, *Materials Today: Proceedings*, 2021, ISSN 2214-7853
- [13] Mishra, A. K., Roy, P., Bandyopadhyay, S., & Das, S. K. (2022). Feature fusion based machine learning pipeline to improve breast cancer prediction. *Multimedia Tools and Applications*, 81(26), 37627-37655.
- [14] Karjadi, D. A., Wedha, B. Y., & Santoso, H. (2022). Heavy-loaded Vehicles Detection Model Testing using Synthetic Dataset. *Sinkron: jurnal dan penelitianteknikinformatika*, 7(2), 464-471.
- [15] Maqsood, S., Damaševičius, R., & Maskeliūnas, R. (2021). Hemorrhage detection based on 3D CNN deep learning framework and feature fusion for evaluating retinal abnormality in diabetic patients. *Sensors*, 21(11), 3865.
- [16] Zebari, D. A., Ibrahim, D. A., Zeebaree, D. Q., Mohammed, M. A., Haron, H., Zebari, N. A., ... & Maskeliūnas, R. (2021). Breast cancer detection using mammogram images with improved multi-fractal dimension approach and feature fusion. *Applied Sciences*, 11(24), 12122.
- [17] Jabeen, K., Khan, M. A., Alhaisoni, M., Tariq, U., Zhang, Y. D., Hamza, A., ... & Damaševičius, R. (2022). Breast cancer classification from ultrasound images using probability-based optimal deep learning feature fusion. *Sensors*, 22(3), 807.
- [18] Tamim, N., Elshrkawey, M., & Nassar, H. (2021). Accurate diagnosis of diabetic retinopathy and glaucoma using retinal fundus images based on hybrid features and genetic algorithm. *Applied Sciences*, 11(13), 6178.
- [19] Gayathri, S., Gopi, V. P., & Palanisamy, P. (2021). Diabetic retinopathy classification based on multipath CNN and machine learning classifiers. *Physical and engineering sciences in medicine*, 44(3), 639-653.
- [20] Asia, A. O., Zhu, C. Z., Althubiti, S. A., Al-Alimi, D., Xiao, Y. L., Ouyang, P. B., & Al-Qaness, M. A. (2022). Detection of Diabetic Retinopathy in Retinal Fundus Images Using CNN Classification Models. *Electronics*, 11(17), 2740.
- [21] Latchoumi, T. P., Swathi, R., Vidyasri, P., & Balamurugan, K. (2022, March). Develop New Algorithm To Improve Safety On WMSN In Health Disease Monitoring. In *2022 International Mobile and Embedded Technology Conference (MECON)* (pp. 357-362). IEEE.
- [22] Reguant, R., Brunak, S., & Saha, S. (2021). Understanding inherent image features in CNN-based assessment of diabetic retinopathy. *Scientific Reports*, 11(1), 1-12.
- [23] Das, S., & Saha, S. K. (2022). Diabetic retinopathy detection and classification using CNN tuned by genetic algorithm. *Multimedia Tools and Applications*, 81(6), 8007-8020.
- [24] Nahiduzzaman, M., Islam, M. R., Islam, S. R., Goni, M. O. F., Anower, M. S., & Kwak, K. S. (2021). Hybrid CNN-SVD based prominent feature extraction and selection for grading diabetic retinopathy using extreme learning machine algorithm. *IEEE Access*, 9, 152261-152274.
- [25] Daanouni, O., Cherradi, B., & Tmiri, A. (2021). Automatic detection of diabetic retinopathy using custom cnn and grad-cam. In *Advances on Smart and Soft Computing* (pp. 15-26). Springer, Singapore.
- [26] El Hossi, A., Skouta, A., Elmoufidi, A., & Nachaoui, M. (2021, May). Applied cnn for automatic diabetic retinopathy assessment using fundus images. In *International Conference on Business Intelligence* (pp. 425-433). Springer, Cham.
- [27] Arumuga Maria Devi, T., & Hepzibai, R. (2022). Clinical Assessment of Diabetic Foot Ulcers Using GWO-CNN based Hyperspectral Image Processing Approach. *IETE Journal of Research*, 1-12.
- [28] Brintha, N. C., Nagaraj, P., Tejasri, A., Durga, B. V., Teja, M. T., & Kumar, M. N. V. P. (2022, June). A Food Recommendation System for Predictive Diabetic Patients using ANN and CNN. In *2022 7th International Conference on Communication and Electronics Systems (ICCES)* (pp. 1364-1371). IEEE.